FR 8102431

9. International conference on high energy physics and nuclear structure. 9. ICOHEPANS.
Versailles,France, July 6 - 10, 1981.
CEA - CONF 5833

# ELECTROMAGNETIC INTERACTIONS ON LIGHT NUCLEI

N. de BOTTON

DPh-N/HE, CEN Saclay, 91191 Gif-sur-Yvette Cedex, FRANCE

Abstract : The field of electromagnetic interactions on light nuclei is reviewed through a discussion of a few topics for which new experimental results have been obtained since the 1979 Vancouver Conference.

## 1. Introduction

The field I am given the opportunity to review is characterized by the unique possibility it provides in nuclear physics, to reach a quantitative description starting from the elementary aspects of the forces between the constituents of the nucleus. The electromagnetic theory is the most accurate theory valid on an extended scale of distances. On the other hand, few nucleon systems properties can be studied in the non relativistic conventional nuclear physics approach by solving exactly a Schrödinger equation for the two-particle interaction. In so far as corrections to this conventional picture of the nucleus are negligible, electromagnetic interaction should give unambiguous answers on the nucleonic currents. The various complications to the simplified version of the nucleus arising because of meson exchange currents, isobar components, relativistic corrections, three-body forces, multiquark admixtures will modify the picture but light nuclei are still the only place where theory can deal quantitatively with these difficulties.

Let us summarize briefly the characteristics of the electromagnetic probe. Electron scattering is described by the diagram on fig. 1. Because of the smallness of the coupling constant the electron exchanges only one virtual photon with

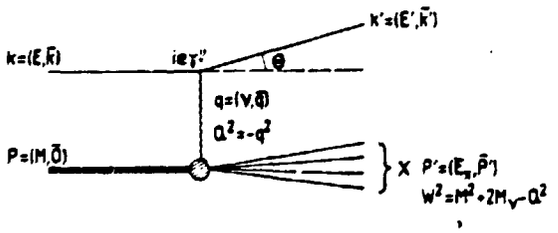


Fig. 1. Single photon exchange Feynman diagram.

the low Z target. The virtual photon emission vertex is exactly known from QED. Recent measurements[1]) of Bhaba scattering ($e^-e^+ \to e^-e^+$) for $s^{1/2}$ up to 31.6 GeV have shown that one can parametrize the form factor of negative electrons by the expression

$$F(q^2) = 1-q^2/(q^2-\Lambda^2)$$

with a value of the cut-off parameter $\Lambda > 95$ GeV. This establishes that electrons

are point-like particles in their electromagnetic interactions down to a radius less than $10^{-16}$ cm. The choice of k' and $\theta$ defines completely the virtual photon and determines the region in space ($\Delta x \sim 1/\sqrt{Q^2}$) and time ($\Delta t \sim 1/E$ excitation) which is explored in the interaction. For instance deep inelastic scattering at large transfer (both $Q^2$ and E excitation are large - $Q^2 > 2\,GeV^2$ ; $W > 2$ GeV - ) allows resolving the quark substructure of the nucleons. On the other hand, elastic scattering ($\Delta t = \infty$) at large transfer ($Q^2 = 8\,(GeV/c)^2$) will be sensitive to average small scale properties of the nucleus like the presence of exotic multiquark admixtures or density fluctuations. By reading the proceedings of the previous ICOHEPANS one gets convinced that the time scale of the evolution of the subject I am discussing is much larger than the two-year interval which traditionally separates two consecutive meetings. As an experimentalist my goal will be to up-date the state of the investigation of some topics for which new experimental results have been obtained since the Vancouver Conference. I will discuss successively experiments which emphasize various aspects of the nuclear dynamics corresponding to increasingly short distance investigation of the nucleus : the classical nucleus picture in quasi elastic(e,e'p) on $^3He$, the meson exchange currents corrections in the electro-magnetic form factors of $^3He$, the propagation of $\Delta$ in nuclei through photon absorption in C and O, and the relevance of quarks in the interpretation of high energy elastic scattering on deuterium. Lastly, I will sketch the possibilities opened by the availability of sources of polarized electrons and the recent progress in polarized targets as demonstrated in a polarized electron on polarized proton experiment. This survey is inevitably non exhaustive and I apologize in advance for the selection of experiments I present, which is biased more because of my deficiencies than by real prejudice. However I volontarily left out of the discussion two subjects which would lose of their importance out of their general context : the observation of anomalies in the photoproduction on deuterium[2], closely related to the existing evidence for dibaryons, and the experiments on the two body photodisintegration of $^3He$ [3] which have to be analyzed within a general account on the possible violation of T invariance.

## 2. Quasielastic (e,e'p) reaction on helium-3

The motivation of (e,e'p) proton knock-out reactions is the measurement of single particle properties of nuclei. Within the frame of the plane wave impulse approximation (PWIA) the cross section of the process sketched in fig. 2 can be factorized according to :

$$\frac{d\sigma}{d\vec{k}'d\vec{p}'} = K \frac{d\sigma^{(p)}}{d\Omega_{e'}} S(\vec{p},\varepsilon) \ ;$$

K is a kinematical factor, $d\sigma^{(p)}/d\Omega_{e'}$ the elastic electron proton cross section including off-shell corrections, and $S(\vec{p},\varepsilon)$ the spectral function which is the probability to find a proton of momentum $\vec{p}$ and removal energy $\varepsilon$ in the initial

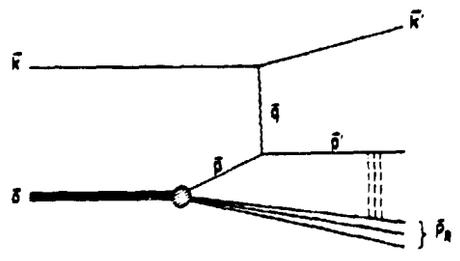


Fig. 2. The (e,e'p) reaction

nucleus. PWIA describes the main features of the process but it is a simplification of the more complex reality : the final state interaction (FSI) of the ejected proton with the residual nuclear state is sizeable even in very light nuclei, mesonic exchange currents (MEC) and isobaric components (IC) in the nucleus wave function bring additional corrections. The factorization of the cross section is no more valid and strictly speaking one cannot anymore extract the spectral function from the data.

The whole picture has been beautifully surveyed in a systematical way by H. Arenhövel[4]) for the (e,e'p) on deuterium. Initially, corrections to PWIA had been overlooked and underestimated leading to a puzzling 20 % discrepancy between theory and experiment[5]). Fig. 3 shows the satisfactory agreement achieved by a recent calculation of Arenhövel for the two different kinematical conditions

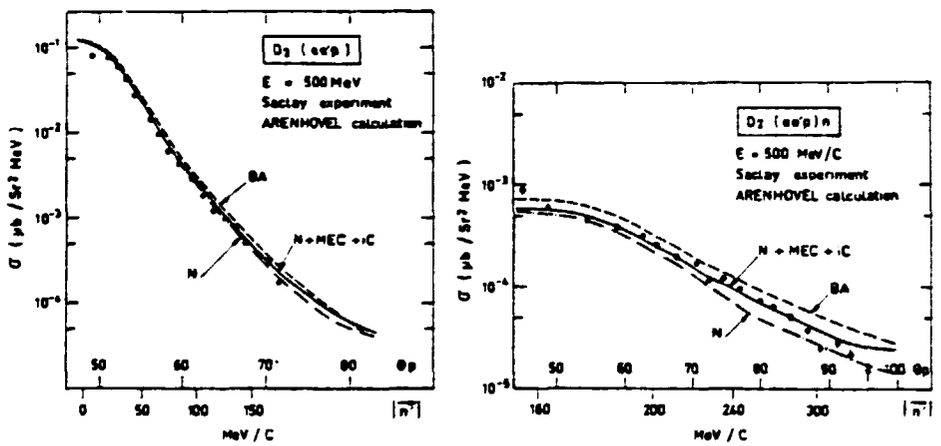


Fig. 3. The (e,e'p) cross-section on deuterium[5]) $d^5\sigma/d\Omega_e d\Omega_p d\nu$ as a function of the recoil momentum, is compared to a calculation by Arenhövel[4]). The dashed line is the PWIA, the dash-dotted line is the Born approximation with final state interaction. The solid line is the complete calculation including meson-exchange currents and isobaric components contributions. The two panels correspond to different kinematics : a) $|\vec{q}| = 450$ MeV/c , b) $|\vec{q}| = 350$ MeV/c

used in the Saclay deuterium experiment[6]). The calculation includes FSI treatment taking into account partial waves up to L = 6, Δ components in the wave function and π, ω and ρ exchange currents.

The $^3$He(e,e'p) coincidence experiments have been carried out at Kharkov[7]) and Saclay[8]). The two-body (e+$^3$He → e'+p+d) and three-body (e+$^3$He → e'+p+p+n) channels are clearly separated in the Saclay experiment thanks to a 1.2 MeV energy resolution in the missing mass spectrum (fig. 4) ; results cover the momentum range out to 300 MeV/c and missing energies up to 90 MeV. The so called "perpendicular kinematics" situation (proton measured in the direction orthogonal to the transferred momentum) has been used.

In the conventional picture of a non relativistic nucleus made of non composite nucleons interacting through a two-body potential , the spectral function of $^3$He can be calculated exactly. Two such PWIA calculations are available, they use a Faddeev approach [9]) and a variational technique[10]) ; both utilize the RSC interaction ; their results essentially differ in the region of low moments (p<100 MeV/c) for which the variational wave function gives a too small contribution. The overall agreement with the effective momentum distributions extracted from the data prealably corrected for radiative

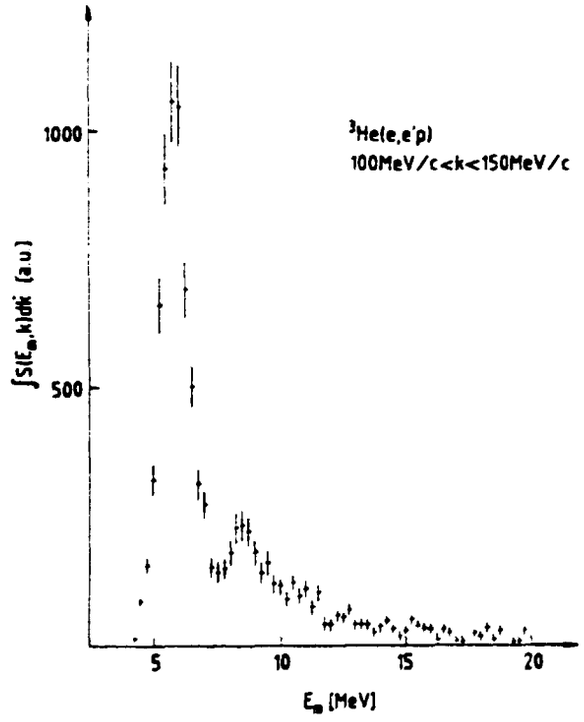


Fig. 4. The missing energy spectrum in the Saclay $^3$He(e,e'p) experiment . The experimental points have been corrected for radiative effects.

effects is satisfactory in the two-body as well as in the three-body channels (figs. 5 a) and 5 b)). However the high quality of the data certainly deserves a confrontation with more detailed calculations including all mentioned corrections : for instance the relative weight of two-body vs. three-body break-up is a quantity very sensitive to the three-body wave function but no meaningful comparison is presently possible.

Clearly an extension of the data to higher momenta (p > 300 MeV/c) would be desirable in the region where inclusive quasi elastic scattering suggests a lack of high-momentum components in the three-body wave functions[11]. Since the signal to accidentals ratio is 0.3 for the 300 MeV/c measurement of the Saclay experiment, this would require in addition to higher electron energy, larger duty cycle accelerators (presently Saclay is 1 % and Kharkov 0.05 %) and more performant detectors achieving a coincidence time resolution less than 1 ns.

Measurement of the four structure functions characterizing the (e,e'p) cross section would necessitate non coplanar experiments that none of the presently available experimental set-ups allow. However by selecting the kinematical conditions a separation of transverse and longitudinal components of the interaction is possible[12], which could enhance meson exchange contributions relatively to single particle ones.

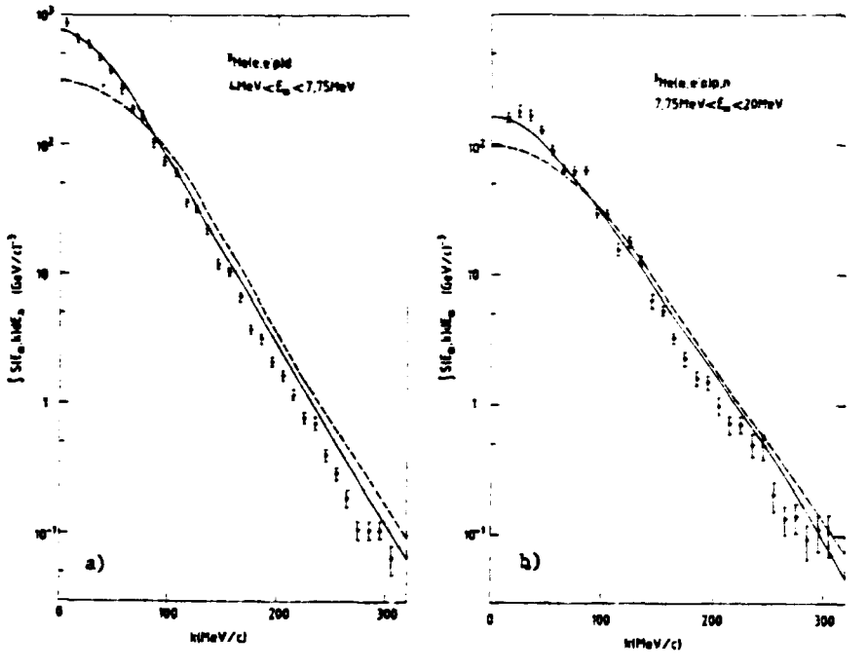


Fig. 5. The Saclay $^3$He momentum distribution[9]) corresponding to : a) the two-body break-up channel, b) the three-body break-up channel, compared to predictions of Dieperink et al.[9]) (solid line) and Cioffi et al.[10]) (dashed line)

## 3. The magnetic form factor of $^3$He

The anomaly in the magnetic moment value of $^3$He has been for a long time one of the clear cut evidences for the existence of meson exchange currents. Low momentum transfer backward electron scattering experiments on $^3$He indicated that MEC dominated the one body contribution for $Q^2 > 5$ fm$^{-2}$. This was shown to happen because of a strong destructive interference between the S and D components of the wave function in the single nucleon current matrix element, reducing significantly the impulse approximation contribution. Owing to this peculiar situation the $^3$He magnetic form factor can be considered as a testing ground for MEC calculations. In this perspective Riska"[7]) has investigated the sensitivity of the overall prediction to the various ingredients entering the form factor calculation.

Recently the old Stanford data[13]) reaching the first diffraction minimum have been superseded by the low transfer high accuracy MIT data[15]). However an extension of the measurements to higher $Q^2$ was desirable in order to study how reliable were MEC calculations in predicting such distinctive experimental features as the position and size of the secondary maximum. The new Saclay measurements[14]) cover the momentum transfer region going beyond the secondary maximum out to $Q^2 = 32$ fm$^{-2}$. The upgraded energy of the Saclay linac was essential in this experiment which used a 700 MeV incident electron beam ; the high intensity (up to 40 μA average current) allowed measuring cross-sections as low as $10^{-38}$ cm$^2$/sr.

In fig. 6 the data are compared to a calculation of Bornais et al.[16]). Owing to the considerable "corrections" to the one-body contribution, the agreement

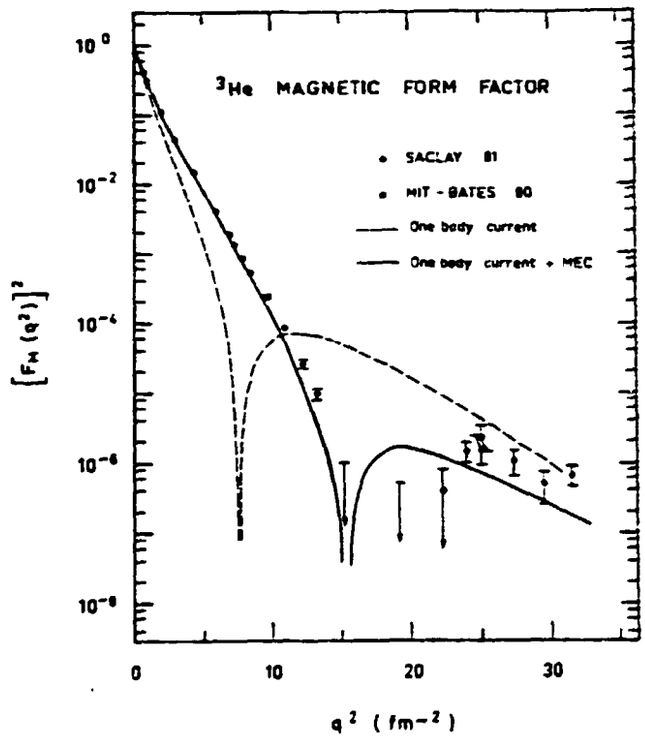


Fig. 6. The $^3$He magnetic form factor. Experimental data from MIT[15]) and Saclay[14]) are compared to calculations from R. Bornais et al. [16]).

with the data is satisfying, it proves that MEC calculations are now under control throughout the momentum transfer region experimentally studied. The calculation is part of a complete investigation by these authors of the electromagnetic form factors of $^3$He and $^3$H ; this is important in view of the requirement of explaining the whole set of 3-body nuclei properties within the same coherent frame. The three-body Faddeev Grenoble wave-function for the Reid soft core potential is used ; a detailed estimation of the exchange processes for $\pi$,$\rho$ and $\omega$ mesons is made which includes form factors to account for the spatial extension structure of the meson-nucleon vertices. Understanding MEC contributions in the magnetic form factor is a prerequisite for their investigation in the charge form factor where they appear as corrections of relativistic order $1/M^2$ and where their theoretical foundation is much less firmly established. The $^3$He charge form factor calculation by the same authors displayed in fig. 7 is in general agreement with the trend of the experimental data for $Q < 6$ fm$^{-1}$, however it underestimates the experimental results below the first minimum. The pair NN processes for $\pi$,$\rho$ and $\omega$ exchange are essential in reproducing the data in the region of the secondary maximum ; they can be considered as part of the relativistic corrections since they naturally appear in a relativistic impulse approximation treatment. Many uncertainties still exist ; let us point out especially the insufficient knowledge of the nucleon form factors which plagues the interpretation of nuclei form factors for $Q > 4$ fm$^{-1}$.

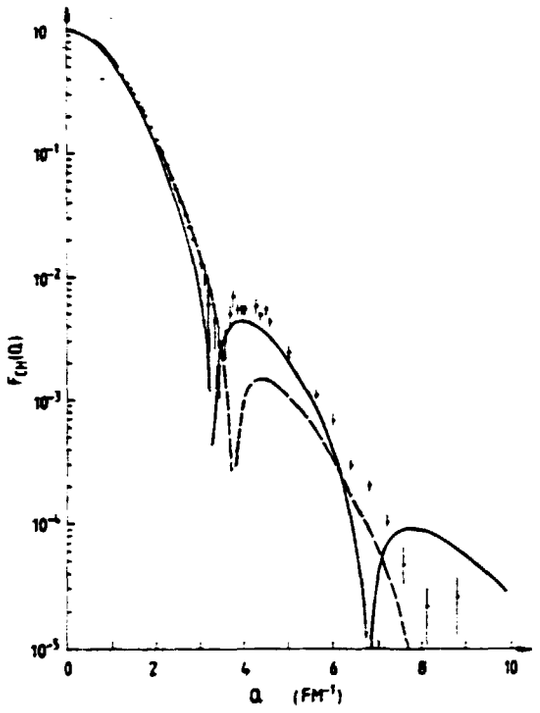


Fig. 7. The $^3$He charge form factor. Data points from ref.[*9])compared to a calculation of R. Bornais et al.[16]). One-body density (dashed line), total (solid line).

Hajduk et al.[17]) have investigated in a detailed way the effect of the Δ isobar components (IC) in the three nucleon bound state properties and especially in the electromagnetic form factors. The IC give rise to a three-body force in addition to specific MEC currents. The Δ contributions (fig. 8) are evaluated


Fig. 8. One-body diagrams involving a Δ isobar explicitly present in the wave-function.

using a wave function solution of the Faddeev equation which includes the single Δ configurations generated nonperturbatively by a realistic transition potential. In the case of the magnetic form factor all Δ contributions are shown to cancel out up to $Q^2$=25 fm$^{-2}$ ; however large π and ρ pair current exchange corrections improve significantly the agreement with the data ; other important exchange corrections are in the process of being calculated[19]). Of special interest for the $^3$He charge

form factor are the non diagonal Δ contributions which correspond to a bound nucleon deformation decreasing the density at the center of the nucleus. A recent evaluation[17]) of these contributions gives a result much too small to explain the features of the secondary maximum in variance with a previous estimate reported at the Vancouver Conference[18]). In fact diagonal Δ contributions cancel the non-diagonal Δ contributions in the secondary maximum region and the only net effect is caused by the polarization of the purely nucleonic components induced by the presence of the Δ isobar.

Summarizing, within the uncertainties we quoted, the corrections to the conventional nucleus picture in a non relativistic frame , seem by and large to account for the main features of the $^3$He magnetic form factor up to $Q^2 = 35\ fm^{-2}$. There are still difficulties in reproducing the charge form factor and the large number of theoretical ingredients involved makes difficult to clearly ascertain each specific correction.

## 4. Photonuclear and electronuclear reactions on light nuclei in the Δ resonance region.

Pion photoproduction on nucleons is known to be dominated by the Δ(1236) resonance ; its amplitude is well described by a resonant M1 contribution in addition to Born terms. Photon induced reactions on deuterium in the region of the Δ resonance have been extensively studied these last years both experimentally and theoretically [20]). Most of the experimental features have been reproduced by a model in which one considers in addition to the quasi-free process the various pion-nucleon and nucleon-nucleon rescatterings. Usually processes up to order 2 in this multiple scattering series are sufficient to account for the data. The few unexplained experimental facts have been considered either as manifestation of genuine ΔN scattering effects or as an indication of the existence of exotic dibaryonic states. In view of the overall success of the model it seems very appealing to extend the method to the interpretation of photoreaction data on heavier nuclei. However effects like the coherent propagation of the Δ in the nucleus can render the multiple scattering series very slow to converge. It may thus become more convenient to solve for the Δ resonating part of the process, the eigenvalue problem of the hamiltonian of a system of (A-1) nucleons and one Δ[21]). In this frame the reaction amplitude for the resonance mechanism reads

$$T = \sum_{\mu} F^{d}_{\mu}(k_x)\ \frac{1}{\omega - \varepsilon_{\mu}}\ F^{e}_{\mu}\ (\omega,q)$$

where $F^{e}_{\mu}(\omega,q)$ describes the excitation by virtual photon $(\omega,q)$ of the eigenmode $\mu$, of energy $\varepsilon_{\mu}$, which propagates and eventually decays with emission of particle x, with momentum k, according to the matrix element $F^{d}_{\mu}(k_x)$. Inclusive reactions (total, virtual or real photon absorption) will essentially study the excitation properties of the resonant amplitude, whereas exclusive reactions (photoproduction of pions and nucleons) will give information on the decay features of these resonances.

Total absorption photonuclear cross-sections for light nuclei in the Δ region can be measured by different methods. We will sketch briefly their main characteristics in order to emphasize the originality of the recent Bonn measurements[22]) which have provided us with a wealth of exclusive and inclusive data on nuclei ranging from He to Pb.

1. In the attenuation method used by the Mainz group[23]), the attenuation caused by a thick target is determined by the target in target out ratio of the photon spectrum measured in a Compton spectrometer. The total absorption is corrected from the calculated electronic absorption to get the nuclear absorption cross-section. Measurements utilizing this method are limited by the ratio of nuclear to electromagnetic cross sections which varies approximately like 1/Z and by the theoretical uncertainties in the calculation of the electronic cross-section. With the present Mainz accelerator duty cycle measurements for nuclei heavier

than carbon are almost impossible.
2. Measurements of deep inelastic electron scattering in the Δ region when extrapolated to the photon point ($Q^2 = 0$) yield the total photoabsorption cross section. The cross sections have to be corrected from radiative effects (both elastic and inelastic) and for the quasi elastic contribution ; these corrections induce uncertainties which grow with the nucleus charge and depend on the kinematical conditions. Extrapolation to the photon point requires determination of the double differential electron scattering cross section at different low values of the transfer momentum. Results using this method have been obtained for a few nuclei including H, D, C and Al. [24]).
3. In the high-energy method, used by the Bonn group[22]), one takes advantage of the difference in the angular distributions of the forward peaked electromagnetic cross section and the almost isotropic nuclear cross section. Tagged bremsstrahlung photons are used ; the hadronic counters surrounding the target detect and identify charged pions and protons and a shower counter vetoes the electromagnetic events (see fig. 9). Double differential cross sections are measured in the angular region going from 20° to 140°, and the energy thresholds for pions and protons are respectively 40 MeV and 58 MeV. In order to deduce the total absorption nuclear cross section from these data, corrections must be applied to account for the energy threshold and finite solid angle of the hadronic counter as well as for the non-detected neutral channels. An intranuclear cascade computer code determines in the case of the Bonn experiment that the ratio of observed to total events grows approximately from 0.4 to 0.8 in light nuclei (Be, C, O) when photon energy varies from 200 MeV to 400 MeV.

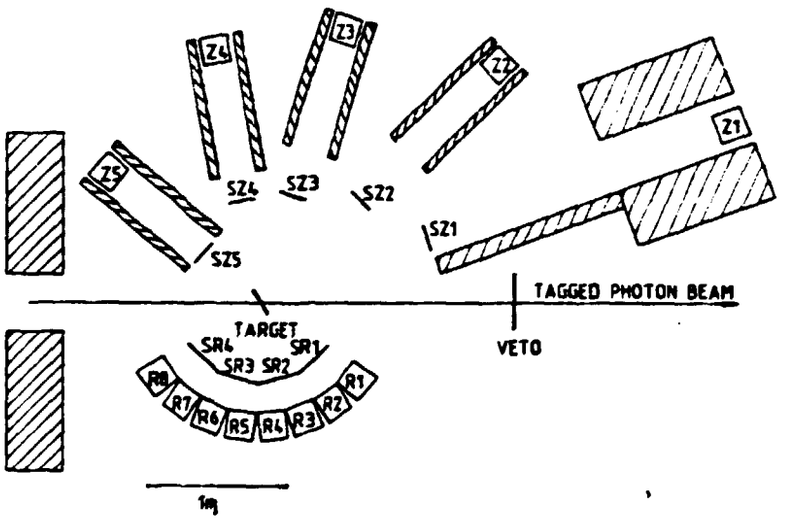


Fig. 9. The Bonn experimental set-up for measurement of photoemission of charged pions and protons[22])

Data obtained on Be using methods 1 and 3 are in perfect agreement within the experimental errors (see fig. 10). On the other hand the old deep inelastic electron scattering data of Kharkov on C strongly disagree with the recent Bonn measurements : Kharkov cross sections are 100 % larger at 200 MeV and 25 % larger at 400 MeV ; this conflicting situation should certainly be an incentive for new electron scattering measurements especially to test the extrapolation procedure at the photon point.

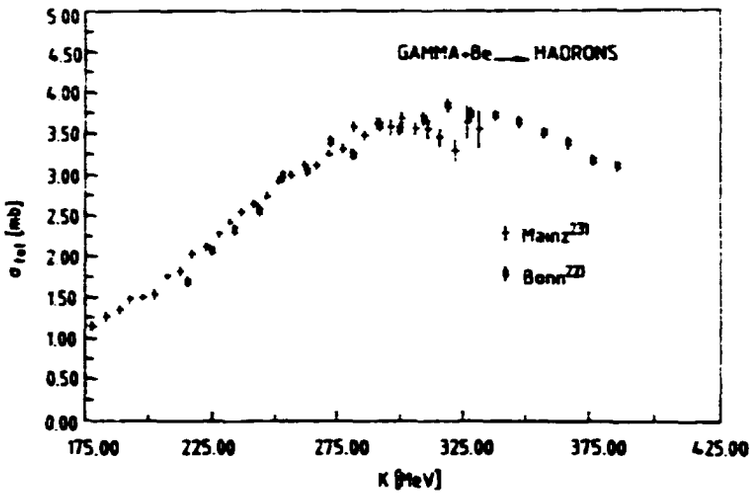


Fig. 10. Total hadronic Be cross section. Data are from ref. 22 and ref. 23.

In fig. 11 we show a sample of the carbon Bonn data[25]) and compare them to the predictions of Laget[26]). The proton spectrum (fig. 11 a)) exhibits a two peak structure : the lower energy peak corresponds to quasi-free pion photoproduction kinematics whereas the high energy peak is associated to a quasi-deuteron process. The quasi deuteron contribution compares reasonably well, after correcting for proton absorption (damping by a factor 0.8), to an estimation (solid line) which is a variation of the Levinger quasi-deuteron model, $\sigma = L\,NZ/A\,\sigma_D$ : the cross section is proportional to the number of neutron proton pairs in the nucleus, and to the $\rho$ and $\pi$ meson exchange part of the deuteron photodisintegration cross section ; the factor L/A accounts for the difference in density of a neutron proton pair in nucleus A as compared to deuterium ; the value L = 10 is suggested by photoabsorption data below pion threshold. The dashed line is the contribution of the quasi free pion photoproduction.

The pion spectrum (fig. 11 b)) displays a bump connected to single pion quasifree photoproduction (dashed line); the size and the shape of this contribution are well reproduced by taking into account the quasi elastic scattering of the emitted pion with the residual nucleus by means of an optical potential (solid line). The low energy part of the spectrum can be associated to inelastically scattered pions.

The total cross section for $\pi^+$ emission (fig. 11 c)) has a shape which differs from the free nucleon cross section (dotted line): the energy shift and the broadening of the resonance are attributed to the binding and to the Fermi motion of the nucleons. Including these effects in a distorted wave impulse approximation (dashed line) and correcting for true absorption of pions, Laget almost reproduces the measured cross section.

The total cross section for proton emission (fig. 11 d)) is compared to the incoherent sum (solid line) of quasifree photoproduction $p\pi^0$ and $p\pi^-$ (dashed line) and exchange quasi-deuteron cross section (dotted line).

The total photoabsorption cross section (fig. 11 e)) is then compared to the incoherent sum (solid line) of pion photoproduction ($\pi^0$, $\pi^+$, $\pi^-$) (dashed line) and exchange contributions approximated by the quasi-deuteron model (dotted line). In view of the simplicity of this semi-phenomenological model the resulting cross section describes surprisingly well the general shape and size of the experimental data.

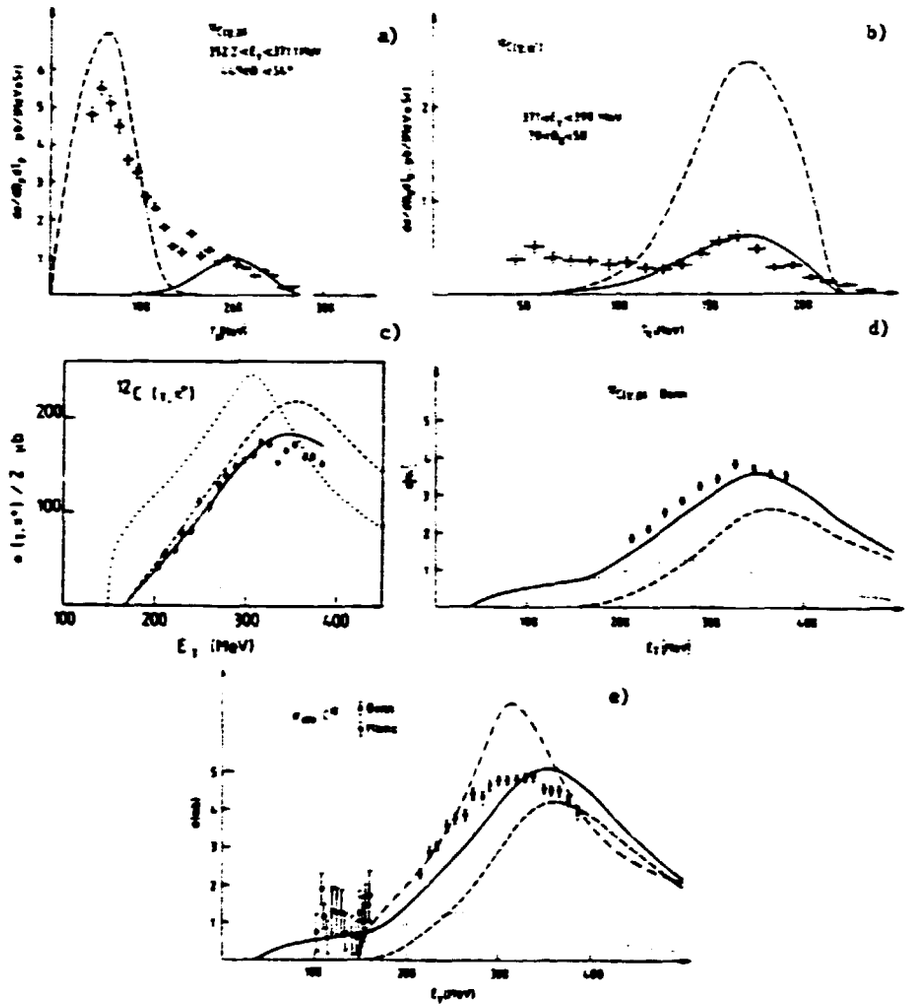


Fig. 11. Photoproduction on $^{12}C$; the experimental Bonn data [22]) are compared to calculations of Laget[16]) (symbols are explained in the text).

In fig. 12 the $^{16}O$ total photoabsorption cross section [22]) is compared to a detailed calculation of Weise and Oset[27]) who used the alternative approach of the Δ-hole microscopic model to describe the resonant part of the process. The total photoabsorption cross section is related through to optical theorem to the imaginary part of the forward photon elastic scattering amplitude. The coherent multiple scattering of pions is mediated by a one-pion exchange Δ-hole interaction ; however the authors observe that the coherent *forward* propagation of photoproduced pions is strongly suppressed because of the transverse nature of γNΔ coupling. The Δ-hole states width and position are thus only moderately modified from the free decay properties and this mainly because of binding effects and Fermi motion. Corrections associated to the Δ propagation in the nucleus medium (Pauli blocking and true absorption NΔ → NN) produce a net slight broadening of Δ-hole

states. The non resonant parts of the cross section (Born photoproduction and El quasi deuteron) have been added incoherently to the resonant part.

In conclusion, we could say that the lack of coherence of the Δ propagation in photoabsorption explains the success of the semi-phenomenological model of Laget which describes the process in terms of one-body and two-body currents in the nucleus.

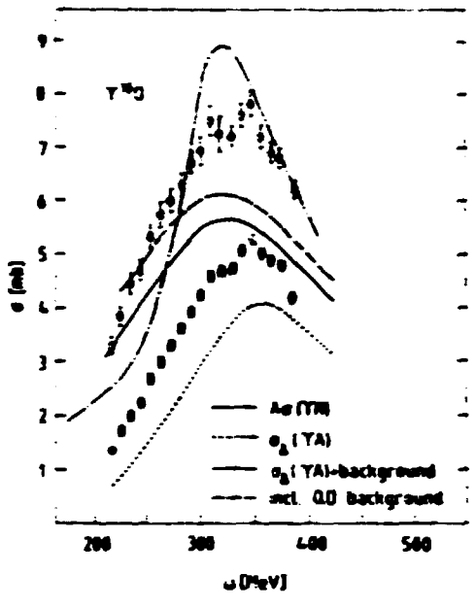


Fig. 12. Total $^{16}O$ photoabsorption cross-section. Data from ref. 22 are compared to a calculation by Oset and Weise[27]. Lower points are the measured cross section for emission of charged particles ; higher points are the extrapolated total absorption cross section.

Deep inelastic inclusive electron scattering in the Δ region is a reaction analogous to photon absorption : instead of real photons the nucleus absorbs virtual photons. Measurements at forward angles and momentum transfers $Q^2 = 0.2 - 0.4\ (GeV/c)^2$ showed no deviations from a model describing the process as an incoherent superposition of single nucleon processes[28].

In fig. 13 we present the results of a Saclay experiment on $^{12}C$ [29]) for comparable momentum transfer but for a scattering angle of 145°. The dip predicted by an impulse approximation between the quasi elastic and the quasi free pion production is filled by an extra contribution. In addition we observe that the resonance peak is shifted and broadened as in the case of real photoabsorption.

The inelastic electron scattering cross section can be expressed in terms of the two response functions $S_L(Q^2,\nu)$ and $S_T(Q^2,\nu)$ corresponding respectively to the longitudinal and to the transverse component of the exchanged virtual photon, which contain the information on the structure of the target

$$\frac{d^2\sigma}{d\Omega dE'} = \left(\frac{d\sigma}{d\Omega}\right)_{Mott} \left\{ \left(1+\frac{\nu^2}{Q^2}\right)^{-2} S_L(Q^2,\nu) + \left[\frac{1}{2}\left(1+\frac{\nu^2}{Q^2}\right)^{-1} + tg^2\frac{\theta}{2}\right] S_T(Q^2,\nu) \right\}.$$

Mesonic exchange current contributions are mainly induced by transverse photons ;

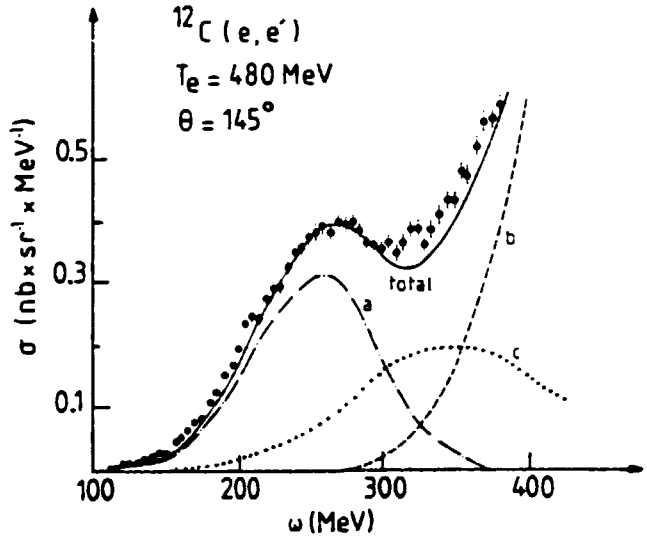


Fig. 13. $^{12}C(e,e')$ differential cross section as a function of the excitation energy $\omega$ at backward angle. Data from Saclay[20]) are compared to a calculation by Laget[26]). Quasi elastic (dash-dot), quasi free pion electroproduction (dash), exchange contribution (dot) and total (solid line).

they will preferentially show up for large scattering angle experiments. We compare the Saclay data to a calculation by Laget [26]) using essentially the same ingredients than in the case of photoabsorption ; the dip between the quasi elastic and the quasi free pion production is filled by the meson exchange contributions approximated in the quasi-deuteron model.Klingenbeck and Huber[21]) give an alternative interpretation of the general trend of the experimental data in terms of the excitation of $\Delta^*$ resonances.

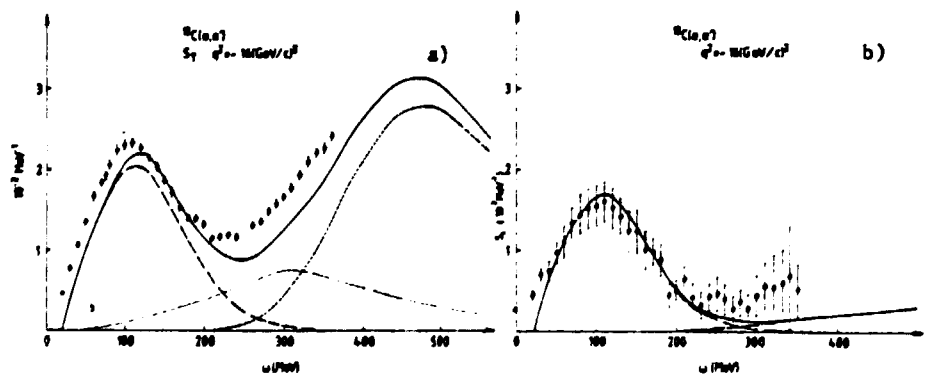


Fig. 14. The transverse (a)) and longitudinal (b)) response functions of $^{12}C$ at $Q^2 = 0.16$ (GeV/c)$^2$ as a function of the excitation energy $\omega$. Data from ref. [28]) are compared to a calculation by Laget [26]). Quasi elastic (dash-dot), quasi free pion electroproduction (dash), exchange contribution (dot) and total (solid line).

By measuring the cross section at different angles a separation of the longitudinal and transverse response functions has been achieved. The two response

functions are displayed in fig. 14 where they are plotted as a function of the excitation energy $\omega$ for $Q^2 = 0.16$ (GeV/c)$^2$. Meson exchange currents scarcely contribute to the longitudinal response function which can be thus used to study short range properties of the nuclear wave function. Unfortunately because longitudinal electroproduction cross section is much smaller than the transverse one, its knowledge requires difficult experiments as witnessed by the size of the error bars. On the other hand the transverse response function is useful for the investigation of MEC.

## 5. Inclusive eD scattering at $Q^2 = 8$ (GeV/c)$^2$

The transition from the classical model of a nucleus made of nucleons, amended by the introduction of mesonic exchange currents and isobaric components, to the quark and gluon picture of the nucleus is certainly one of the most important problems we are presently facing. To investigate this issue we must identify nuclear properties which require in order to be explained the explicit consideration of the quark degrees of freedom of the nucleon. In that respect high energy electron scattering measurements on light nuclei performed at SLAC by the American University Group are apparently the most promising and relevant experiments. Arnold et al.[29] present new inelastic data in the threshold region for deuterium, $^3$He and $^4$He.

In the case of deuterium preliminary results extend to $Q^2 = 8$(GeV/c)$^2$ the explored momentum transfer region (see fig. 15).

In terms of the two inelastic structure functions $W_1(Q^2,W)$ and $W_2(Q^2,W)$ the inelastic cross section for electron scattering at angle $\theta$ may be written :

$$\frac{d\sigma}{d\Omega dE'} = \left(\frac{d\sigma}{d\Omega}\right)_{Mott} \left[W_2(Q^2,W) + 2W_1(Q^2,W)\ tg^2\ \theta/2\right]$$

where $Q^2$ and W are the squared quadritransfer and the invariant mass of the final hadronic state.

For elastic scattering, using the two elastic structure functions $A(Q^2)$ and $B(Q^2)$ the cross section reads :

$$\frac{d\sigma}{d\Omega} = \left(\frac{d\sigma}{d\Omega}\right)_{Mott} \left[A(Q^2) + B(Q^2)\ tg^2\theta/2\right].$$

At forward angles, it is essentially the structure functions $A(Q^2)$ and $W_2(Q^2,W)$ which are measured.

Using their previous lower $Q^2$ data[30] the authors were able to show that the inelastic to elastic structure function ratio is almost independent of $Q^2$ at fixed missing mass W for $Q^2 > 2$(GeV/c)$^2$ and $W-M_D < 200$ MeV

$$\frac{W_2(Q^2,W)}{A(Q^2)} = C(W^2). \qquad (1)$$

Such a connection is also predicted by a parton model analysis of the threshold region[31].

From the inelastic threshold data values of the elastic structure function $A(Q^2)$ were deduced using relation (1) at $Q^2 = 6$(GeV/c)$^2$ (where previous measurements yielded only an upper limit of A) and at $Q^2 = 8$(GeV/c)$^2$. In view of the comparison with theoretical models these two indirectly determined new data points are extremely important since they reach the expected domain of validity of scaling models $Q^2 >> M_D^2$. A detailed comparison of these experimental results with the various existing models is beyond the scope of this review (and the ability of the speaker) ; I will limit myself to sketch some of the calculations which are the

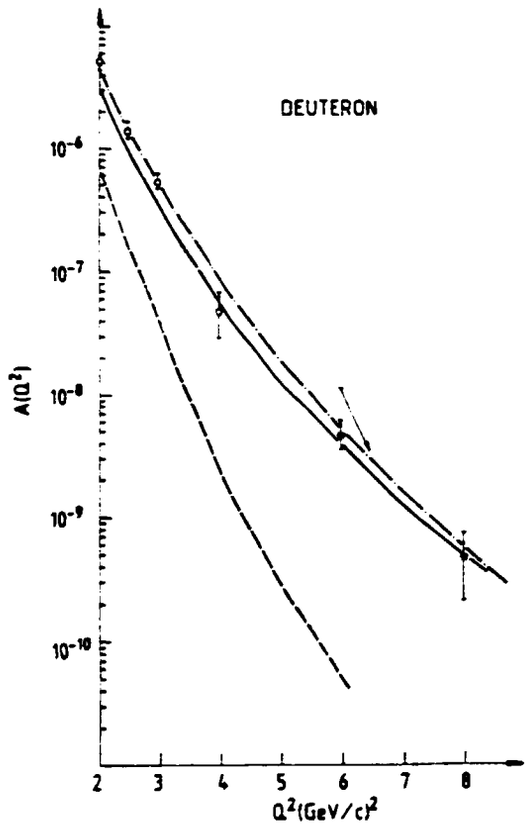


Fig. 15. Elastic scattering structure function A for deuterium. Data from ref.[29]) (* deduced data, ϕ previous data) are compared to calculations of Arnold et al.[32]) (dash), Brodsky et al.[31]) - quark interchange model - (dash-dot) and M. Chemtob[35]) - T = 2 - (solid line).

most representative of the different approaches adopted by the theorists.

Clearly a fully relativistic treatment is a must at these very high momenta. The recent analysis of Arnold et al.[32]) is made in a language familiar to nuclear physicists ; the relativistic impulse approximation contribution is calculated using a four component wave-function which includes negative energy nucleon states. Various wave functions corresponding to different nucleon nucleon potentials were used. All results underestimate the structure function A, they predict a quicker fall off than the one exhibited by the data. This would imply that meson exchange contributions should dominate at high $Q^2$. Since pair current terms are automatically included in RIA, other exchange currents should govern the process ; $\rho\pi\gamma$ contributions are expected to be very large at high $Q^2$ but no relativistic evaluation of MEC is presently available. Let us note that in a contribution to this Conference, Bhalerao and Gurvitz[33]) attribute the failure to reproduce the data to the use made by Arnold et al. of the so-called Gross prescription according to which the spectator nucleon is set on-shell. By relaxing this condition and allowing both nucleons to be on-shell with equal probability they obtain a perfect agreement with the experimental values. This conflicting situation can be solved by more elaborate calculations using expansions of the Bethe Salpeter equation.

From the point of view of the dimensional scaling quark model (DSQM)[31]) based on the relevance of the quark compositeness of the nucleus, the form factor A has an asymptotic behaviour $\sqrt{A} \sim (Q^2)^{-5}$. This law reflects that, for high mo-

mentum transfers, binding corrections can be neglected. In order to leave intact the deuterium nucleus, the momentum transfer should be equipartitioned among the six constituent quarks. The amplitude for transferring to each constituent the momentum Q/6 is $\alpha_s/(Q/6)^2$ where $\alpha_s$ is the QCD coupling constant. The scaling expected by the DSQM is apparently observed to occur for $Q^2 \geq 3(GeV/c)^2$. Let us not however that DSQM predicts only the asymptotic fall off power law and not the normalization of $A(Q^2)$ which would require knowledge of the amplitudes of the various short lived multiquark components admixed to the two nucleon component. This limitation is somewhat unsatisfactory since no prediction is made about the onset of scaling.

QCD predicts in addition to the nucleonic and isobaric components of the deuterium wave function, "hidden color" states which correspond to two color-octet three-quark clusters, the overall state being a color singlet[36]). In terms of the 6 valence quarks

$$|D> = a|(uud)_{1c}(ddu)_{1c}> + b|(uud)_{8c}(ddu)_{8c}>$$

$$+c|(uuu)_{1c}(ddd)_{1c}> + d|(uuu)_{8c}(ddd)_{8c}>.$$

According to the color nature of the state the dominant scattering mechanism is different. Since nucleons cannot exchange one single gluon, the quark interchange model is relevant for the part of the wave function corresponding to two color singlet three quark clusters, whereas the democratic chain model is pertinent for the color octets three-quark clusters (fig. 16). The preasymptotic scaling law differs according to the involved mechanism. The data tend to favor the quark interchange prediction ; the expression

$$A \sim C_D \frac{F_N(Q^2/4)}{1+Q^2/m^2}$$

with $C_D = 0.15$ and $m^2 = 0.28\ GeV^2$, reproduces the data from $Q^2 = 0.7\ (GeV/c)^2$ to $Q^2 = 8\ (GeV/c)^2$ (dash-dotted curve in fig. 15).

A nucleon parton approach suggested by Schmidt and Blankenbecler[34]) considers phenomenological constructs in the infinite momentum frame which should join smoothly to the nuclear non relativistic wave function allowing standard normalization of the charge form factor at $Q^2 = 0$. Chemtob[35]) incorporates to this treatment the spin degrees of freedom which increase the number of predicted quantities. The results are very sensitive to the postulated binding forces characterized by the power index T (T = 1 scalar meson exchange, T = 2,3 vector meson exchange with and without form factor at the vertices). The case T = 3 which has an alternative interpretation in terms of a three valence-quark structure of the nucleon considerably underestimates the form factor A at large $Q^2$ ; on the other hand the T = 2 prediction reproduces the elastic scattering data cut to $8\ (GeV/c)^2$ without any arbitrary normalization. This would tend to suggest that the quark degrees of freedom are not yet relevant in this transfer region and that binding corrections to a different asymptotic law could simulate the $(Q^2)^{-10}$ behaviour in the preasymptotic region. However the same T = 2 wave function gives too small predictions for the inelastic structure function $\nu W_2$, indicating that we cannot reach for the moment definite conclusions. Let us note that as for the case of the $^3He$ charge form factor, there are important uncertainties induced by the insufficient knowledge we have of the nucleon electric form factors at high momentum transfer.

Lastly, allowing percentages of six quark admixtures in the deuteron wave function induces large contributions on the elastic form factor at high $Q^2$ which could be used to revelate these exotic components[37]).

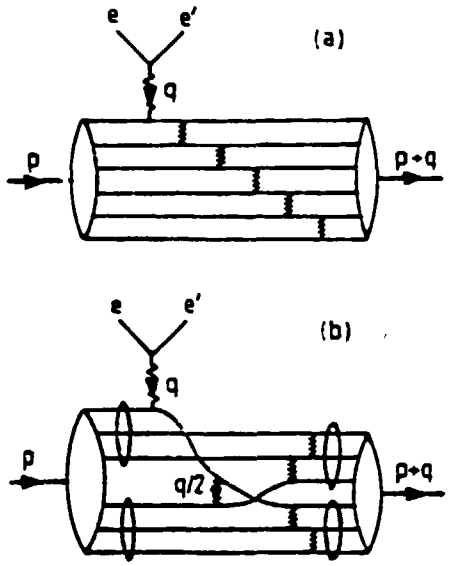


Fig. 16. Possible mechanisms contributing to the deuteron elastic form factor for large $Q^2$. (a) democratic chain, (b) quark interchange.

## 6. Polarized electron scattering on polarized protons

I will present now an experiment which may be is slightly out of the domain covered by this Conference. However, I think that it is important to us because it demonstrates that some experiments involving polarization are presently feasible thus opening the field of spin nuclear physics with the electromagnetic probe. This potentiality has been made reality by the advent of polarized electron sources and by the progress on polarized targets which both rely on advanced techniques in condensed matter and atomic physics. The Yale group experiment[38]) at SLAC utilized the Peggy I [39]) polarized electron source which is based on the principle of photoionization of aligned $^6$Li atoms. The polarization of the electron beam was 80 % and the intensity was typically 60 μA. Peggy I was preferred to the Peggy II source, based on the photoemission from a semi conductor (Ga As) illuminated by polarized light, which was utilized for the parity-violation experiment[40]) (polarization : 40 %, intensity : several hundreds of mA), because of the radiation damage produced on the proton polarized target by the high beam intensity. The problem of finding radiation resistant materials for polarized targets is central to the development of polarized experiments. The butanol-porphyrexide polarized "proton" target operating on the principle of dynamic nuclear polarization had a 1/e depolarizing dose of $3 \times 10^{14}$ e/cm$^2$ ; it required annealing every three hours and subsequent repolarization. This severe limitation is presently being surmounted : recent experiments at SLAC [41]) have shown that the rediation damage to ammonia ($NH_3$) is significantly less than for butanol (1/e depolarizing dose larger than $10^{16}$ e/cm$^2$). For a discussion on recent progress achieved on polarized electron sources and polarized targets we refer to the Proceedings of the Lausanne Symposium on polarization[42]).

What follows is intended to give some insight in the kind of new information polarized experiments can produce. For instance inelastic electron scattering of longitudinally polarized electrons off polarized protons allows investigating two new spin dependent structure functions $G_1(\nu,Q^2)$ and $G_2(\nu,Q^2)$.

The quantity measured by the Yale group experiment at SLAC is the asymmetry

$$A = \frac{\frac{d^2\sigma}{d\Omega dE'}^{\uparrow\downarrow} - \frac{d^2\sigma}{d\Omega dE'}^{\uparrow\uparrow}}{\frac{d^2\sigma}{d\Omega dE'}^{\uparrow\downarrow} + \frac{d^2\sigma}{d\Omega dE'}^{\uparrow\uparrow}} = \frac{M(E-E'\cos\vartheta)\ G_1(\nu,Q^2) - Q^2 G_2(\nu,Q^2)}{W_2(\nu,Q^2) + 2\mathrm{tg}^2\frac{\vartheta}{2}\ W_1(\nu,Q^2)}$$

for deep inelastic inclusive scattering for protons polarized parallel or antiparallel to the incident electron longitudinal polarization. The kinematical range $3.5 < Q^2 < 10\ (\mathrm{GeV/c})^2$ and $2 < W < 5$ GeV was covered.

Because of the 10° forward angle kinematical condition, the quantity essentially measured is the transverse asymmetry

$$A_1 = \frac{\sigma^T_{1/2} - \sigma^T_{3/2}}{\sigma^T_{1/2} + \sigma^T_{3/2}} \sim - \frac{Q^2 G_2 + \nu M G_1}{W_2}$$

for photoabsorption of circularly polarized photons into states with $J_2 = 1/2$ and $J_2 = 3/2$ ($\gamma^{\uparrow} + P^{\uparrow} \to \sigma_{3/2}$ ; $\gamma^{\downarrow} + P^{\uparrow} \to \sigma_{1/2}$). Like $W_1$ and $W_2$, $G_1$ and $G_2$ scale for high $Q^2$ so that $A_1(\nu,Q^2) \to A_1(x)$ where $x$ is the Bjorken scaling variable $x = Q^2/2M\nu$.

In a simple quark-parton interpretation the absorbed virtual photon will necessarily flip the spin of the quark for angular momentum conservation: $\gamma^{\uparrow} + q^{\downarrow} \to q^{\uparrow}$ or $\gamma^{\downarrow} + q^{\uparrow} \to q^{\downarrow}$ ; $\gamma^{\downarrow}q^{\uparrow}$ and $\gamma^{\downarrow}q^{\downarrow}$ cannot interact.

The two transverse cross sections are expressed as

$$\sigma_{3/2} \sim \Sigma q_i^2 f_i^{\downarrow}(x)$$

$$\sigma_{1/2} \sim \Sigma q_i^2 f_i^{\uparrow}(x)$$

where $q_i$ is the charge of quark of flavor i, $f_i^{\downarrow}(x)$ and $f_i^{\uparrow}(x)$ the probability of finding the quark i which carries momentum $xP_{\text{nucleon}}$ with helicity antiparallel or parallel to the proton helicity.

The simplest wave function of a three s-wave valence quarks proton predicts

$$f_u^{\downarrow} = \frac{1}{9} \qquad f_u^{\uparrow} = \frac{5}{9} \qquad f_d^{\downarrow} = \frac{2}{9} \qquad f_d^{\uparrow} = \frac{1}{9}$$

yielding

$$A = \frac{\frac{4}{9}\left(\frac{5}{9} - \frac{1}{9}\right) + \frac{1}{9}\left(\frac{1}{9} - \frac{2}{9}\right)}{\frac{4}{9}\left(\frac{5}{9} + \frac{1}{9}\right) + \frac{1}{9}\left(\frac{1}{9} + \frac{2}{9}\right)} = \frac{5}{9}\ .$$

The preliminary data displayed in fig. 17 do not seem to support this simple view, they indicate that A becomes large for large x suggesting that in this region the spin of the nucleon is carried by the valence quark which carries also the entire momentum of the nucleon.

Elastic scattering and scattering in the resonance region of 6.4 GeV longitudinally polarized electrons off polarized protons were also measured. For instance the elastic scattering asymmetry reads

$$A = \tau \frac{G_M}{G_E}\left\{\frac{2M}{E} + \frac{G_M}{G_E}\left[\frac{2\tau M}{E} + 2(1+\tau)\tan^2\frac{\vartheta}{2}\right]\right\}\left\{1+\tau\left[\frac{G_M}{G_E}\right]^2\left[1+2(1+\tau)\tan^2\frac{\vartheta}{2}\right]\right\}^{-1}$$

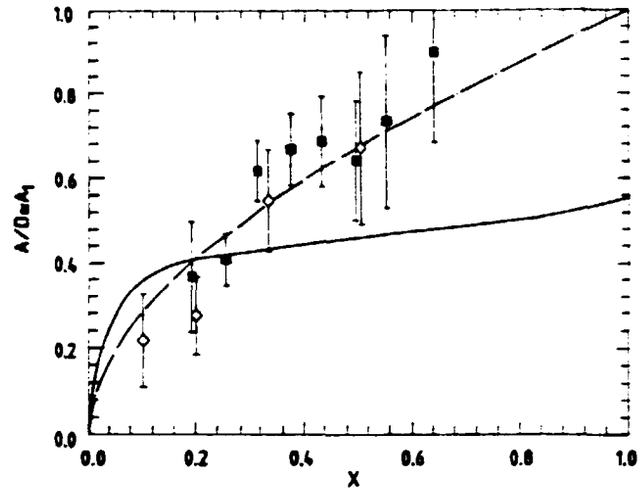


Fig. 17. Deep inelastic asymmetry A1 as a function of the Bjorken variable x. The data from ref.[38]) are compared to theoretical predictions using a symmetrical valence-quark model[45]) of the proton (solid line), and an unsymmetrical model[46]) in which the entire spin of the nucleon is carried by a single quark in the limit $x = 1$ (dash-dot).

in which $\tau = Q^2/4M^2$ and $G_E(Q^2)$ and $G_M(Q^2)$ are the electric and magnetic form factors of the proton.

In principle A can be used to measure the electric form factor of the proton in the region $Q^2 > 2$ GeV$^2$ where $G_E$ is insufficiently known but present low counting rates prevent us from reaching this goal ; it however allowed determining in a previous experiment[43]) the sign of $G_E/G_M$ which is positive as already indicated by the hyperfine structure of hydrogen. An equivalent method for polarized elastic electron scattering has been recently explored by Arnold et al.[44]), these authors propose measuring the recoil polarization by means of a second scattering in order to avoid the difficulties inherent to polarized targets. They calculated counting rates of polarization transfer experiments on hydrogen and deuterium, intended for a determination of the nucleon electric form factors and for the separation of quadrupole and charge form factors of deuterium.

Summarizing, polarized elastic scattering would help measuring through interference terms electric form factors otherwise difficult to reach, and separating form factors for $J \geq 1$ nuclei ; quasi elastic polarized scattering would give insight in the nucleus spin structure. We can thus reasonably hope that by enlarging the number of accessible nuclear properties spin effects should offer new ways of probing theoretical models in greater detail.

Acknowledgements

I would like to express my thanks to Drs. M. Chemtob, B. Chertok, B. Goulard, E. Hadjimichael, B. Mecking, J. Mougey, P. Sauer, Z. Szalata and all my colleagues of the Saclay Linear Accelerator for their cooperation and their help in preparing this report. I am particularly grateful to Drs. J.M. Laget and C. Tzara for many stimulating discussions on the matter of this paper.

References


1) D.P. Barber et al., Phys. Rev. Lett., 43 (1979) 1915.
2) P. P. Argan et al., Communication to this Conference.
3) D.I. Sober et al., Communication to this Conference
4) H. Arenhövel, Perspectives in Electro and Photonuclear Physics, Nucl. Phys. A358 (1981) 263c.
5) J. Mougey, High Energy Physics and Nuclear Structure, Vancouver 1979, Nucl. Phys. A335 (1980) 35.
6) M. Bernheim et al., to be published in Nucl. Phys. A.
7) V.A. Gol'dshtein et al. Yad. Fiz. 27 (1978) 1565 ; Sov. J. Nucl. Phys. 27 (1978) 824 ; Yad. Fiz. 31 (1980) 1388 ; Sov. J. Nucl. Phys. 31 (1980) 796 and Communication to this Conference.
8) E. Jans et al., Communication to this Conference.
9) A.E.L. Dieperink et al., Phys. Lett. 63B (1976) 261.
10) C. Cioffi Degli Atti, Private communication to authors of ref. 8 and Communication to this Conference
11) I. Sick et al., Phys. Rev. Lett. 45, (1980) 871.
12) S. Boffi et al., Communication to this Conference.
13) J.S. Mc Carthy et al., Phys. Rev. Lett. 25 (1970) 884.
14) J.M. Cavedon et al., Communication to this Conference.
15) P.C. Dunn, Thesis Harvard University (1980).
16) R. Bornais et al., Communication to this Conference.
17) Ch. Hajduk et al., Communication to this Conference and Nucl. Phys. A352 (1981) 413.
18) M.M. Giannini et al., Phys. Letters 88B (1979) 13.
19) P.U. Sauer, Private Communication
20) J.M. Laget, Phys. Rep. 69 (1981) 1 and references therein.
21) M.G. Huber and K. Klingenbeck, Perspectives in Electro and Photonuclear Physics, Nucl. Phys. A358 (1981) 243c.
22) J. Arends et al., Phys. Lett. 98B (1981) 423.
23) J. Ahrens, High Energy Phys. and Nucl. Struct., Vancouver 79, Nucl. Phys. A335 (1980) 67.
24) V.G. Vlasenko et al., Sov. J. of Nucl. Phys. 23 (1978) 265.
25) B. Mecking, Private communication.
26) J.M. Laget, Private communication.
27) E. Oset and Weise, Perspectives in Electro and Photonuclear physics, Nucl. Phys. A358 (1981) 163c.
28) P. Barreau et al., Communication to this Conference and private communication.
29) R.G. Arnold et al., Communication to this Conference.
30) R.G. Arnold et al., Phys. Rev. Lett. 35 (1975) 776.
W.P. Schütz et al., Phys. Rev. Lett. 38 (1977) 259.
31) S.J. Brodsky and B.T. Chertok, Phys. Rev. D14 (1976) 3003
32) R.G. Arnold et al., Phys. Rev. C21 (1980) 1426.
33) R.S. Bhalerao and S.A. Gurvitz, Communication to this Conference
34) R. Blankenbecler and I.A. Schmidt, Phys. Rev. D15 (1977) 3321 and D16 (1977) 1318.
35) M. Chemtob, Nucl. Phys. A336 (1980) 299 and Perspectives in Electro and Photonuclear Physics, Nucl. Phys. A358 (1981) 57c.
36) S.J. Brodsky and G.P. Lepage SLAC Pub. 2595 (1980)
37) V.V. Burov et al., Communication to this Conference.
38) G. Baum et al. Communication to the XX International Conference on High Energy Physics, University of Wisconsin (1980).
39) M.J. Alguard et al., Nucl. Instr. and Meth. 163 (1979) 29.
40) C.Y. Prescott et al., Phys. Lett. 77B (1978) 347 and Phys. Lett. 84B (1979) 524.
41) M. Seely et al. (private communication)
42) High Energy Physics with Polarized Beams and Polarized Targets, Birkhäuser 1981, Ed. L. Joseph, J. Sopper.
43) M.J. Alguard et al. Phys. Rev. Lett. 37 (1976) 1258

44) R.G. Arnold et al.,Phys. Rev. C23 (1981) 363.
45) J. Kuti and V.F. Weisskopf, Phys. Rev. D4 (1971) 3418.
46) J. Kaur, Nucl. Phys. B128 (1977) 219.
47) D.O. Riska, Nucl. Phys. A350 (1980) 227.
48) U. Glawe et al., Phys. Lett. 89B (1979) 44.
49) J.S. McCarthy et al., Phys. Rev. C15 (1977) 1396 ;
R. Arnold et al., Phys. Rev. Lett. 40 (1978) 1429.